Experimental investigation of multistage electrodialysis for seawater desalination

Desalination 464 (2019) 105–114

Contents lists available at ScienceDirect

Desalination

journal homepage: www.elsevier.com/locate/desal

Experimental investigation of multistage electrodialysis for seawater desalination

G.J. Doornbusch[a,b], M. Tedesco[b], J.W. Post[b], Z. Borneman[a], K. Nijmeijer[a,*]

[a] Membrane Materials and Processes, Department of Chemical Engineering and Chemistry, Eindhoven University of Technology, P.O. Box 513, 5600 MB Eindhoven, The Netherlands

[b] Wetsus, European Centre of Excellence for Sustainable Water Technology, P.O. Box 1113, 8900 CC Leeuwarden, The Netherlands

ARTICLE INFO

Keywords:
Electrodialysis
Multistage
Seawater desalination
Energy consumption
Water transport

ABSTRACT

Electrodialysis (ED) is currently used for selective removal of ions and brackish water desalination, while for seawater desalination ED is considered to be too energy intensive. This research focuses on the viability of ED using multiple stages for seawater desalination. With staging, the driving force is adapted to the governing conditions at that specific stage, operating at its individual optimum at lower energy consumption. An ED multistage configuration is examined that contains up to four stages. We compare single stage with multistage ED and investigate the effect of operation parameters. Different current densities are applied and optimized and residence time is compared to describe both transmembrane salt and water fluxes. We showed that desalination from 500 mM to 200 mM is possible, but that for these desalination conditions a multistage and single-stage system perform equal. Operation of each stage of the multistage close to limiting current density shows that desalination of synthetic seawater close to drinking water quality is possible. To reach this, the energy consumption is 3.6 kWh/m3 and at least 4 stages are needed. Although outlet concentrations between ED and RO are different, this non-optimized ED system showed double the energy consumption of the state-of-the-art desalination technology RO.

1. Introduction

Seawater desalination with reverse osmosis (RO) is increasingly important to meet fresh water demands for the growing population in water scarce regions suffering from increasing periods of droughts [1–4]. Current highly optimized RO systems require an electrical energy input of 2 kWh per m^3 of fresh water produced [2,5–7], which is close to the thermodynamic minimum work of 1.1 kWh per 1 m^3 of fresh water produced from 2 m^3 of seawater, i.e. at a water recovery of 50% which is typical for a commercial RO process [2].

In RO, over the years energy consumption decreased thanks to the development of higher permeable membranes, more efficient pumps, and highly efficient energy recovery devices [2,8,9]. Elimelech and Philipp calculated that potentially an energy consumption of 1.56 kWh/m^3 could be obtained (using 100% efficient pumps and energy recovery devices, no concentration polarization or frictional losses down the channel, at 25 °C and 50% water recovery). A staged RO system design using an interstage booster pump could in theory bring the actual energy consumption closer to the thermodynamic limit [2].

The use of staging in an alternative membrane desalination technology like electrodialysis (ED) may be considered. Contrary to RO, electrodialysis (ED) is not widely used for seawater desalination yet because ED is considered to be too energy intensive [10,11]. In ED, however, which is an electricity-driven membrane desalination process, staging can be applied and may induce a further reduction in energy consumption, because at each stage, the applied potential difference can be adapted to the governing conditions at that specific stage. The multistage ED configuration can potentially improve the non-homogeneous distribution of ion transport along the flow direction of the stack since separate stages allow different operational conditions. Consequently, each stage can then be operated at its individual optimum, instead of applying conditions that are selected based on the total system optimum.

In industrial processes ED is often operated in a batch configuration, however, in large-scale plants continuous processes are preferred in order to have a continuous supply and quality of water [12,13]. For this reason, Seto et al. suggested to use a continuous multistage ED for seawater desalination but this was not tested experimentally [14]. In fact, a batch process can be considered as an infinite multistaged process, depending on the number of cycles. A two-stage ED configuration

* Corresponding author.
E-mail address: d.c.nijmeijer@tue.nl (K. Nijmeijer).

https://doi.org/10.1016/j.desal.2019.04.025
Received 5 February 2019; Received in revised form 14 April 2019; Accepted 21 April 2019
Available online 01 May 2019

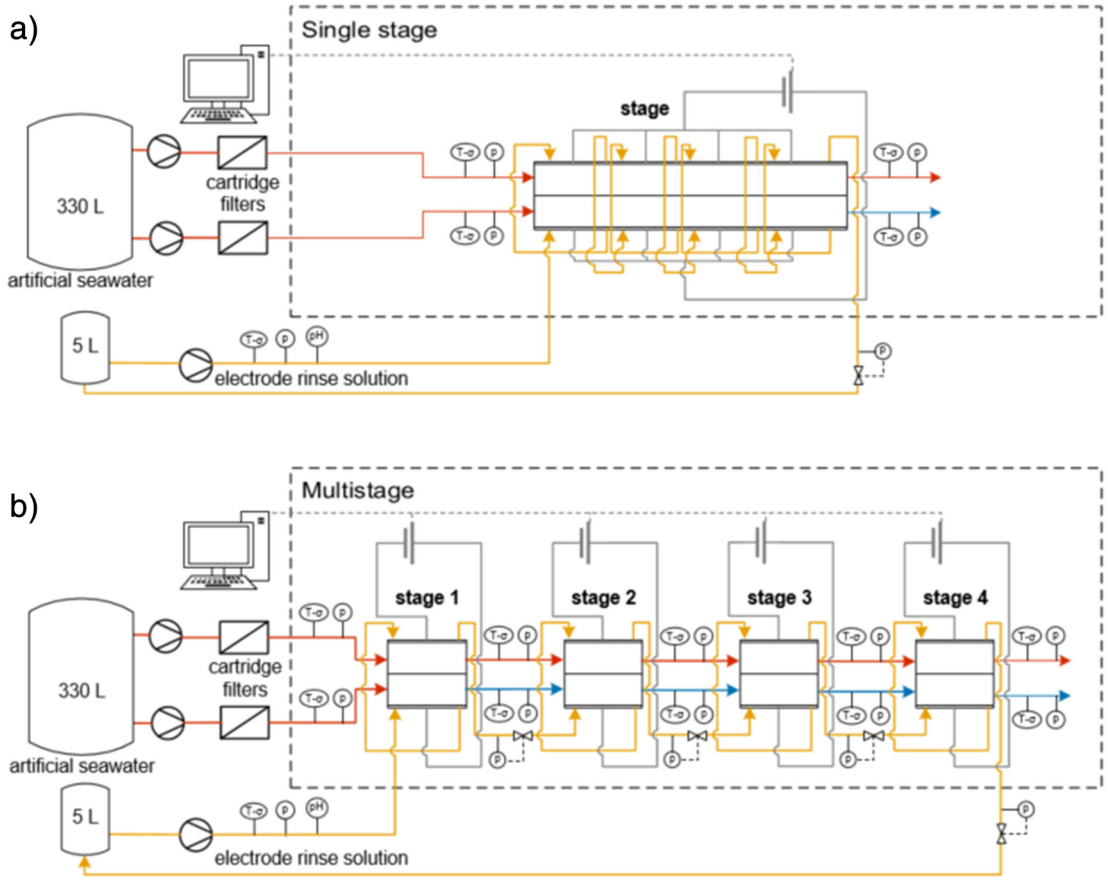

Fig. 1. Schematic representation of the experimental setup: a) single-stage ED configuration; b) multistage ED configuration, with same feed on both sides: the diluate (blue), and concentrate (red). For both configurations, the electrolyte rinse solution (yellow) flows from the anolyte to the catholyte of the first electrode pair and subsequently to the anolyte and catholyte of the next electrode pairs.

used by Turek for seawater desalination, similar to the two-stage RO systems [15], resulted in an energy consumption of 6.6–8.7 kWh/m^3. Although not all details were provided, the high value for energy consumption probably stems from the use of low selective membranes. Unfortunately, also the optimal number of ED stages required to produce the desired drinking water quality at minimum energy consumption was not investigated. Furthermore, the two-stage ED configuration was also not compared with the single-stage operation using the same operational conditions (membrane area, flow rate, current density or voltage).

A two-stage ED configuration modelled by Chehayeb et al. showed a reduction in energy of 29% compared to a one stage setup [16]. This model illustrated the benefits of a multistage operation. However, only desalination until 1 g NaCl/L was considered, which is still twice the salt concentration permitted in drinking water [17]. Especially at lower salt concentrations, the energy consumption to further desalinate the solution increases rapidly due to the decreased conductance of the diluate stream. McGovern investigated a multi-stage system to desalinate high saline streams, however, instead of operating a multi-stage ED system, feed waters were fed multiple times through the same stack [18]. Tanaka developed a model for brackish water desalination in order to predict the desalination performance per stage for a maximum of five stages and to assess the lowest energy consumption for brackish water desalination [19]. However, also in the work of Tanaka, experimental validation was lacking.

In the present work, we advance the work on multistage ED with experimental validation and investigate experimentally the effect of staging in continuous seawater desalination ED on desalination performance and energy consumption. Where others have been using only model calculations or batch processes [14] or two-stage ED configurations [15] without making a comparison to a single-stage seawater desalination, we investigated both single and multistage layouts and measure the desalination performance at different experimental conditions. We described the mechanism of mass transport (ions and water) and current utilization per stage by varying the applied current, voltage and the different feed flow velocities. In addition, we determined the limiting current density (LCD) per stage for different feed flow velocities in order to find the maximum desalination rate per stage and to evaluate the potential of multistage ED for seawater desalination.

2. Transport mechanisms in ED

The ion transport through ion exchange membranes (IEMs) in any electro-driven process can be divided in two transport mechanisms, i.e. electro-migration and (back)diffusion. The applied current induces ion migration through the membranes from the diluate to the concentrate, which results in desalination of the diluate. Meanwhile, the obtained concentration gradient over the membranes induces some (back)diffusion in opposite direction, from the concentrate to the diluate, which results in efficiency losses [20–22].

When the driving force is large and therefore the electro-migration is large, a salt depleted boundary layer develops in the diluate compartment at the membrane interface, also referred to as concentration polarization. The driving force at where the concentration of the boundary layer reaches zero is referred to as LCD. At this point the energy consumption increases dramatically and undesired phenomena (electro convection and water splitting) start to play a role [23].

Next to the salt transport through the membranes, water transport

through the membranes can also result in efficiency losses. Water transport can also be specified in two transport mechanisms, i.e. osmosis and electro-osmosis. The concentration gradient raised over the membranes as a result of the desalination process is the driving force for osmosis, due to which water diffuses from the diluate to the concentrate. Along with every ion, a shell of water molecules around the ion is transported through the membrane from the diluate to the concentrate, also referred to as electro-osmosis [24–26]. These effects combined represent the efficiency losses of the desalination process and therefore result in a lower desalination performance, as measured in the experimental set up.

3. Experimental setup and procedure

3.1. Electrodialysis stacks in single-stage and multistage configuration

For the single-stage configuration, one stack was used with an active membrane area of $100 \times 400\,mm^2$ and a total membrane area of $1.41\,m^2$. For the multistage configuration, we used four serially connected stacks with an active membrane area of $100 \times 100\,mm^2$ each and a total membrane area for the multistage of $2.15\,m^2$. The overall layout of both configurations is presented in Fig. 1.

All ED stacks (REDstack B.V., The Netherlands) used consisted of ten cell pairs with the same membranes and gasket-integrated spacers. The stacks were fed in co-flow. Each cell pair consisted of one anion exchange membrane (AEM) and one cation exchange membrane (CEM). In addition, extra AEM shielding membranes were placed adjacent to each electrode in order to prevent leakage of electrode rinse solution. Fujifilm membranes (AEM type 10 and CEM type 10 Fujifilm Manufacturing Europe B.V., The Netherlands) were used because of their low resistance and high permselectivity. The membrane properties as provided by the manufacturer are listed in Table 1.

As shielding AEMs Fumasep FAB-PK-130 membranes (Fumatech GmbH, Germany) were used because of their proton blocking properties in order to maintain pH < 2 in the electrode compartment. The distance between adjacent membranes was fixed by gasket integrated woven spacers of 0.155 mm in thickness with a porosity of 79% (Deukum GmbH, Germany).

The endplates of the stacks contained titanium electrodes (mesh size $1.8\,m^2/m^2$) coated with Ru/Ir mixed metal oxide (Magneto Special Anodes B.V., The Netherlands) with an area of $98 \times 98\,mm^2$. For the multistage configuration, each endplate contained one electrode. For the single-stage configuration, each endplate contained four electrodes of $98 \times 98\,mm^2$ that were electrically operated as a single electrode. The shielding membrane and the endplate were separated using a 0.5 mm silicon gasket (Eriks B.V., The Netherlands), while the electrode compartments were filled with a woven PETEX 07-670/52 spacer (Sefar AG, Switzerland).

The ED configurations were fed with a 510 mM NaCl solution, representing the salinity of seawater. This solution was prepared using demineralized water and technical-grade NaCl (Regenit, Frisia Zout B.V., The Netherlands). The feed water was pumped through the ED configurations with the same feed flow velocity at both the diluate side and the concentrate side using diaphragm pumps (Grundfos DDA220, Denmark). The pulsation of the pumps was levelled out by using a pulsation damper (PDS250 PVC/FKM, Prominent GmbH, Germany). The resulting outlet flow rates were measured for both diluate and concentrate at the outlet of the last stage. The corresponding water flux through the membranes was calculated from the flowrate measurements.

The electrodes were rinsed by recirculating an aqueous solution containing 0.5 M $FeCl_2$, 0.5 M $FeCl_3$, and 0.5 M NaCl, using a flow rate of 340 mL/min by a peristaltic pump (Masterflex, USA). The sodium chloride was added to the electrolyte in order to avoid a large concentration gradient for sodium over the shielding membranes. The pH was monitored (Endress & Hauser GmbH, Germany) and kept below pH 2 by manual addition of 37 wt% HCl. For every experiment at different operational conditions, fresh electrode rinse solutions were employed.

3.2. Electrical instrumentation and sensors

The conductivity was measured inline (VStar22, Thermo Fisher Scientific, USA) at the inflow of the diluate and concentrate stream of the first stage and at the outflow of the diluate and concentrate stream of each stage (Fig. 1b). The pressure was measured (MIDAS SW, JUMO GmbH, Germany) at the same location as the conductivity. The voltage on the working electrodes was measured using a digital multimeter (34461A, Keysight Technologies, USA). The electrical potential or current was applied using individual power sources for every stage (stages 1–3: SM330-AR22 and stage 4: SM70-AR24, Delta Electronika B.V., The Netherlands).

3.3. Experimental procedure

The performance of the single-stage and the multistage configuration were tested and the water transport and salt transport were measured. Table 2 shows the operational conditions applied. The experiments were carried out at different linear feed flow velocities, $v = 5$, 10, 15 and 20 mm/s. Firstly, a uniform current density on all the electrodes was applied in both the single-stage and the multistage configuration. Secondly, for the multistage configuration, it was tested how desalination occurs operating the electrodes with different current densities. A non-uniform current distribution was applied with the highest current density applied to the first stage, followed by a decreasing current density in every subsequent stage. The values of current densities were chosen based on preliminary estimation of optimal values to reach a constant voltage for all the stages.

Next, also the maximum desalination degree per stage in the multistage configuration was investigated by assessing the limiting current density (LCD) per stage and the effect of feed flow velocity on the desalination rate. The maximum desalination degree per stack was determined just before the system reached the LCD. The LCD value was assessed per stage for the feed flow velocities, $v = 2.5$, 5, 10, 15 mm/s and for a maximum of four stages. The LCD was determined by increasing the current density stepwise and measuring the resulting voltage. For the first stage, steps of 10 A/m^2 were used, for subsequent stages, stage two, three and four, the steps were 2.5 A/m^2. The set time for the current density was at least 100 times the residence time of the solution in the stage. The LCD value was found using the Cowan and

Table 1
Properties of ion exchange membranes (data provided by the manufacturer).

	Permselectivity[a] [%]	Water permeability [mL/m²·h·bar]	IEC [meq/g]	Resistance[b] [Ω·cm²]	Thickness (dry) [μm]
Fujifilm AEM type 10	96.0	8	2.85	1.29	146
Fujifilm CEM type 10	97.6	8	2.90	2.02	155
Fumatech AEM FAB-PK-130	> 95	n/a	0.8	< 4	130

[a] Based on the membrane potential measured over the membrane between 0.05 M and 0.5 M KCl solutions at 25 °C.
[b] Measured in a 0.5 M NaCl solution at 25 °C.

Table 2
Operational conditions for both uniform current and non-uniform current regimes.

	Feed flow velocity [mm/s]	Current density [A/m^2]					
Current condition		Stage 1	Stage 2	Stage 3	Stage 4	Average over Stages	Single-stage
Uniform current	5, 10, 15, 20	25	25	25	25	25	25
	5, 10, 15, 20	50	50	50	50	50	50
	5, 10, 15, 20	75	75	75	75	75	75
Non-uniform current	10, 20	150	75	50	25	75	n.a.
	10, 20	300	150	75	50	144	n.a.
95% of limiting current	2.5, 5, 10, 15	[a]	[a]	[a]	[a]	t.b.d.	n.a.

[a] Experimentally investigated.

Brown method [27,28]. Prior to the determination of the LCD of each subsequent stage, the current density of the preceding stage was set to 95% of the measured LCD value.

For all experiments the voltage reading is corrected for the blank resistance which accounts for the resistance of the electrodes, rinse solution, single shielding membrane and electrical connections. In this case the voltage refers only to the electric potential applied to the membrane pile. Subsequently, the voltage is plotted per cell pair.

4. Results and discussion

First, we compare the single-stage and the multistage configuration for uniform current distribution. The changes in salt concentration are compared by varying the feed flow velocity and the current density. In addition, the salt and water fluxed are compared for both systems. And besides that, we compare the single-stage and multistage configuration for coulombic efficiency and energy consumption at a uniform current operation.

Second, we investigate the current distribution, by comparing for both the single-stage and the multistage effect of current distribution on energy consumption. Uniform and non-uniform current distributions are tested. To reach full desalination we investigate the LCD per ED stage and assess the maximum desalination rate, operating at 95% LCD in each stage for a range of different feed flow velocities.

4.1. Single-stage ED and multistage ED

Fig. 2a shows the change in salt concentration of the diluate from inlet to outlet for both single-stage and multistage configuration as function of the feed flow velocity for different current densities. Fig. 2b shows for both configurations the concentrate inlet-outlet concentration difference as function of the feed flow velocity. Fig. 2c shows the corresponding overall water flux from diluate to concentrate for different feed flow velocities and current densities. Fig. 2d shows the salt flux for different feed flow velocities and current densities as calculated from the concentration change in the diluate obtained from Fig. 2a and the volumetric change obtained from Fig. 2c.

4.1.1. Changes in salt concentrations

Fig. 2a and b shows for both the single-stage and multistage configuration the same trends for the change in concentration of the diluate and the concentrate, respectively. With increasing feed flow velocity the change in salt concentration in both diluate and concentrate decreases because less salt is transported due to the shorter residence time in the system. Increasing the current density leads to an increased salt transport. Hence, a higher change in diluate and concentrate concentration is observed due to the higher driving force applied. Consequently, the salt flux from diluate compartment to concentrate compartment is larger (see also Fig. 2d). Overall, the multistage configuration shows about the same concentration changes as the single-stage configuration. For a given feed flow velocity, each increase in current density results in a similar increase in concentration difference. The amount of salt transported seems to scale directly with the amount of charge supplied. This is also confirmed when the combined effect of feed flow velocity and current density is reviewed for data points which have the same current density over flow rate ratio, i.e., 25 (current density, A/m^2):10 (feed flow velocity, mm/s), 50:20; and 25:5, 50:10, 75:15. In these sets of data points about the same amount of charge has been transferred by the electrodes to the ED stacks, i.e. 40 C and 80 C, respectively. The resulting diluate removal concentrations with limited charge transfer (40 C) are about equal (for the multistage 76 mM, for the single-stage 82 mM). Also at the higher charge transfer (80 C), both diluate removal concentrations are about the same (for the multistage 152 mM, for the single-stage 157 mM). It was not possible to apply a current density of 75 A/m^2 at a feed flow velocity of 5 mm/s in order to get an almost complete desalination ($\Delta C \sim 500$ mM; electrical charge transfer of 240 C) due to reaching limiting current conditions. For the multistage configuration, only the fourth stage was not able to operate at 75 A/m^2, while it was possible to operate the first three stages at 75 A/m^2. From this, we observe that neither a single-stage ED nor a multistage configuration with uniform distribution of current to all the stages reaches full desalination.

4.1.2. Salt and water fluxes

The concentration changes in the diluate and concentrate result from water and salt transport through the membranes from diluate to concentrate and from concentrate to diluate. Transport of both is presented as function of feed flow velocity for different current densities in Fig. 2c and d, respectively. The trends for these fluxes for the multistage and single-stage configurations are similar.

Higher current densities give higher migration rates of hydrated salt ions from diluate to concentrate, and hence, also the electro-osmotic water flux is higher. For a given current density, an increase in feed flow velocity leads to a slight decrease in water flux (Fig. 2c) and a slight increase in salt flux from diluate to concentrate (Fig. 2d). The higher the feed flow velocity, the lower the residence time, and consequently less desalination occurs at the same current density. Therefore, the concentration gradient over the membranes is smaller and is present for shorter time. As a consequence, the driving force for both salt and water diffusion is lower, i.e., the osmotic water flux from diluate to concentrate is lower as well as the back diffusion flux of salt ions from concentrate to diluate (resulting in a net increase of the salt flux from diluate to concentrate). However, at higher feed flow velocity, concentration polarization is less severe as well. In brackish water desalination typically feed flow velocities of 20–40 mm/s are applied in order to limit concentration polarization [10]. For seawater desalination applications, however, concentration polarization may be less relevant due to the higher salt concentrations resulting in higher diffusion fluxes from the bulk solution to the boundary layer.

The multistage configuration clearly shows a higher water flux and a slightly lower salt flux under most conditions tested. Ion migration flux and associated electro-osmotic water flux are in principle similar in both systems, because the current density determines the ion migration flux, so the difference must be attributed to differences in ion diffusion flux and osmotic water flux. The latter two are dependent on current distribution and residence time distribution. Contrary to the current

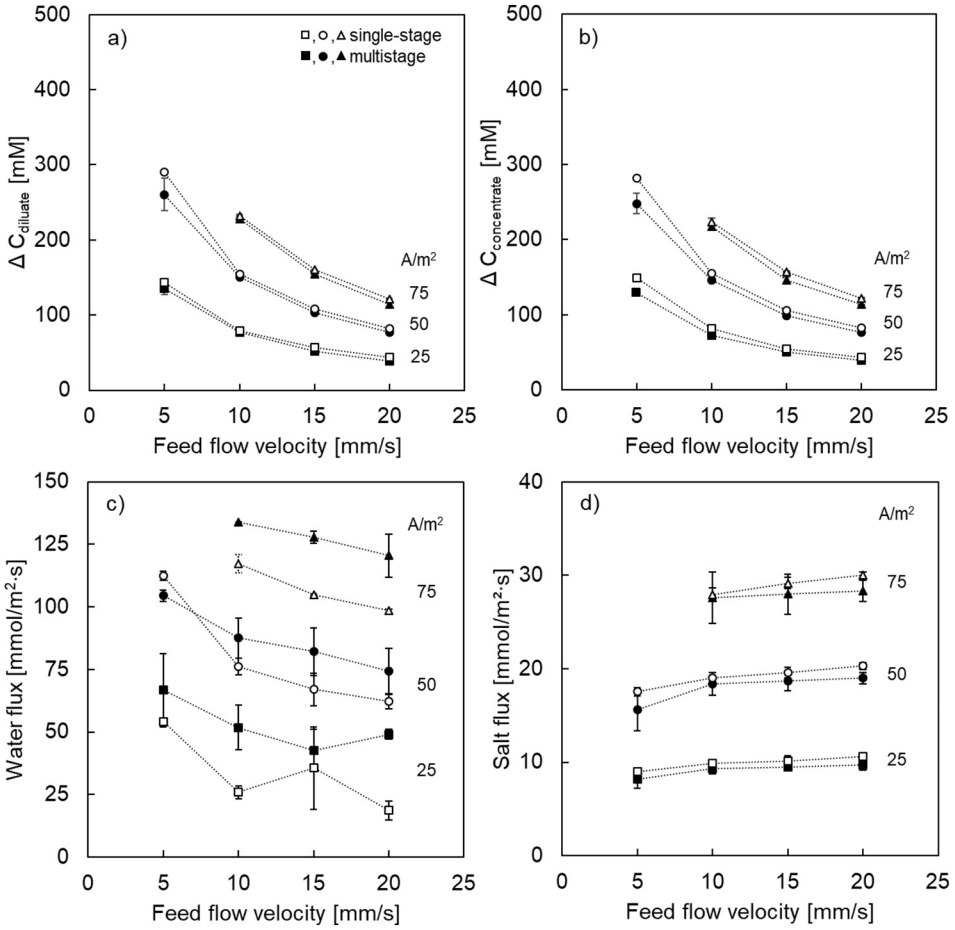

Fig. 2. Effect of feed flow velocity and current density for both single-stage (open markers) and multistage ED (solid markers) on: a) inlet-outlet concentration difference for diluate; b) inlet-outlet concentration difference for concentrate; c) water flux; d) salt flux. The standard deviation for some data points is not visible since it is within the size of the marker. The dashed lines are added to guide the eye.

distribution in the multistage configuration where all the small stacks are operated at a certain current density, the current in the long single-stage configuration may be distributed unequally over the length of the stack. This means ion migration near the inlet is probably higher than near the outlet, and hence the concentration gradient as driving force for back diffusion and osmosis is present for longer times in the single-stage configuration. That means that the current distribution cannot be the explanation by the lower water flux and higher salt flux in the single-stage configuration. Another possibility is that the residence time in the multistage configuration is higher than that in the single-stage configuration. This difference may be caused by the flow pattern near the inflows and outflows at each stage in the multistage ED configuration, whereas the single-stage ED configuration has only one inflow and one outflow.

4.1.3. Coulombic efficiency and energy consumption

For the single-stage and multistage configuration the effect of both feed flow velocity and current density on coulombic efficiency and energy consumption are investigated. The coulombic efficiency is defined as the charge transferred by ions through each membrane from diluate to concentrate divided by the electric charge transferred by the electrodes. The energy consumption is defined as the product of applied currents and voltages during a given time period divided by the volume of diluate outflow produced during that same time period.

Fig. 3a shows the coulombic efficiency as function of feed flow velocity for different current densities. Fig. 3b shows the energy consumption as function of feed flow velocity for different current densities. Fig. 3c shows the measured voltage per cell pair for the single-stage and per stage of the multistage configuration as function feed flow velocity when a current density of 50 A/m^2 is applied. Fig. 3d shows for both configurations the energy consumption as function of the obtained diluate concentration for different feed flow velocities and current densities. The thermodynamic curve provided in Fig. 3d is calculated assuming equal amounts of concentrate and diluate, ideal behaviour of the 500 mM NaCl solutions and assuming perfect selective membranes (i.e., without back diffusion and water transport).

Fig. 3a shows a higher coulombic efficiency at higher feed flow velocities because of the shorter time for water diffusion and back diffusion of salts. In addition, the coulombic efficiency seems to decrease with increasing current density. However, this is misleading since with increased current densities at each feed flow velocity a higher degree of desalination is obtained as observed before in Fig. 2a. Therefore, the coulombic efficiencies at the same amount of electrical charge transferred (discussion of Fig. 2) are compared, i.e. data points that have the same current density over flow rate ratio, i.e., 25 (current density, A/m^2):10 (feed flow velocity, mm/s), 50:20; and 25:5, 50:10, 75:15, at 40 C and 80 C charge transfer, respectively. These data show an increase in coulombic efficiency with higher current density and higher cross flow velocity, in both single and multistage configuration. The coulombic efficiency is mainly influenced by back diffusion of ions. Two main factors play an important role: i) the concentration gradient over the membrane, which is the driving force for back diffusion of salt ions from concentrate to diluate, and ii) the time available for diffusion [29]. Because we compare data points with the same coulombic charge transferred, the established concentration gradient is the same. That implies that different coulombic efficiencies are observed due to a difference in time for diffusion. Comparing the data points of 40 C show an increase in coulombic efficiency from 25:10 to 50:20. In these experiments, the residence time is respectively 40 and 20 s, therefore a shorter diffusion time leads to higher coulombic efficiencies. Comparing the 80C data points, a large increase in coulombic efficiency is shown from 25:5 to 50:10 and 75:15. Between the latter two data points a minor

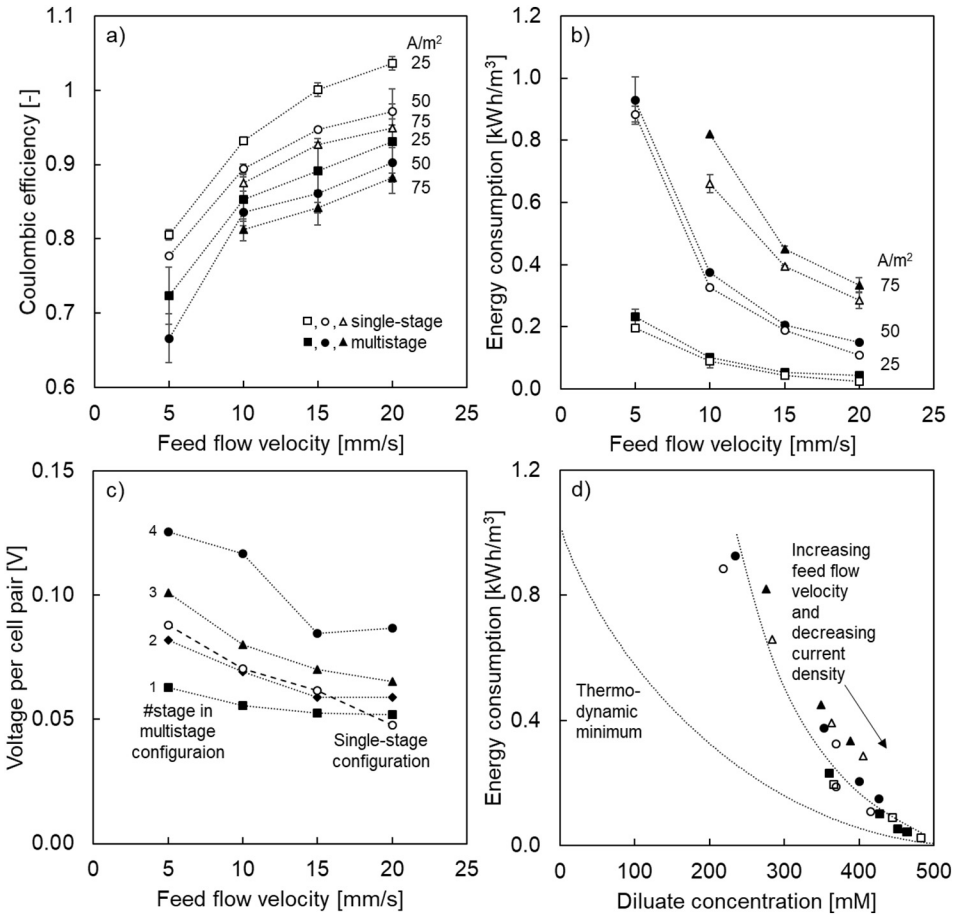

Fig. 3. For both single-stage (open markers) and multistage ED (solid markers) effect of feed flow velocity for (different) current densities on: a) Coulombic efficiency; b) energy consumption; c) voltage per cell pair for 50 A/m^2; d) energy consumption as function of diluate concentration. The standard deviation for some data points is not visible since it is within the size of the marker. The dashed lines are added to guide the eye.

increase is shown, due to small difference in residence time (40 s per stage compared to 27 s), compared to the first point (80 s residence time). When we compare data points with equal coulombic charge transfer, we observe the same behaviour between the single-stage and multistage configuration. From this we conclude that high coulombic efficiencies are obtained at short residence times (i.e. high feed flow velocities).

In general, the multistage configuration has lower coulombic efficiency than the single-stage configuration. As discussed previously, this is most probably due to a higher residence time distribution due to the additional inflow/outflow manifolds in the multistage configuration. Ionic shortcut currents or shunt currents have a detrimental effect on the coulombic efficiency [13,30]. The multistage configuration contains more manifolds compared to the single-stage configuration, attributing to the lower coulombic efficiency of the multistage configuration.

Fig. 3b shows that with increasing feed flow velocity the energy consumption for both the single-stage and the multistage configuration decreases. Due to the shorter residence time at higher feed flow velocities, fewer salt ions are transported from the diluate compartments to the concentrate compartments (Fig. 2a). Increasing the current density leads to an increased energy consumption per m^3 diluate produced, because a higher degree of desalination is obtained (Fig. 2a). The higher the degree of desalination, the higher the concentration gradient over the membranes and the higher the back diffusion. Also, higher degree of desalination results in higher internal resistance, mainly due to the presence of less ions causing an increase of the electrical resistivity of the diluate compartments. Comparing data points with the same coulombic charge transfer, i.e. with about the same desalination degree, also shows that with higher current density the energy consumption is higher, because at a higher current density more energy is dissipated with the faster ion transfer. The trends of energy consumption for single-stage and multistage configurations are similar, although the multistage configuration uses for all current densities slightly more energy. This can be attributed to the lower coulombic efficiency (Fig. 3a) as well as to the higher water transport (Fig. 2c) in the multistage configuration.

Fig. 3c shows the voltage needed per cell pair for the four stages of the multistage and for the single-stage to operate at 50 A/m^2 at different feed flow velocities. With increased feed flow velocity the voltage decreases because the amount of salt transported is smaller due to the shorter residence time resulting in a smaller concentration gradient over the membranes therefore lower voltages. For the lowest feed flow velocity of 5 mm/s, the single-stage configuration requires a voltage in between the voltage needed for the second and for the third stage of the multistage configuration. At higher feed flow velocities, the voltage of the single-stage configuration becomes comparable to the voltage applied to the second stage of the multistage configuration (for 15 mm/s) or to that of the first stage (for 20 mm/s). From this we conclude that for mild desalination (a decrease of the diluate salt concentration from 500 mM towards 200 mM), a multistage configuration with a uniform current distribution has no advantage over a single-stage configuration. For full desalination this will be investigated further below.

Fig. 3d shows the energy consumption for each data point provided in Fig. 3b as function of the diluate concentration. The lower the diluate concentration that is obtained, the higher the energy consumption. As expected, the energy consumption at a given diluate concentration obtained with low current density and low feed flow velocity is lower than with high current density and high feed flow. The energy consumption for the different settings follows the same trend as the curve representing the thermodynamic minimum energy consumption for a reversible desalination (left dashed line in Fig. 3d) [31]. However, due to non-ideal behaviour (i.e. back diffusion and water transport) of the

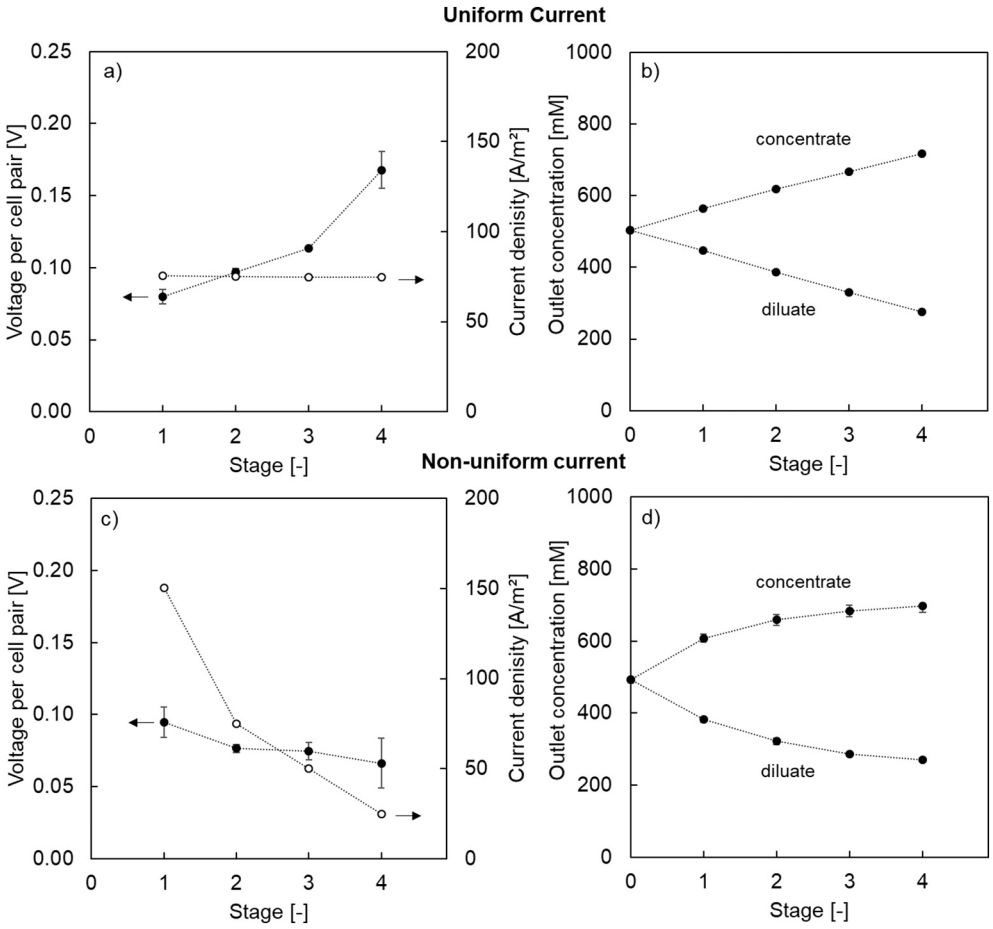

Fig. 4. Effect of uniform current per stage of the multistage on: a) Voltage per cell pair (solid markers) and current density (open markers); b) corresponding outlet concentrations. Effect of non-uniform current per stage of the multistage on: c) voltage per cell pair (solid markers) and current density (open markers); d) corresponding outlet concentrations. The average current density applied to the stages was 75 A/m^2 and the feed flow velocity was 10 mm/s. The standard deviation for some data points is not visible since it is within the size of the marker. The dashed lines are added to guide the eye.

system, the measured energy consumption is larger.

4.2. Effect of current distribution on energy consumption in multistage ED

In this section, the effect of the distribution of the current density is investigated for two different regimes in the multistage ED configuration. The first regime has a uniform current distribution, i.e. each consecutive stage of the multistage is operated at the same current density as in the previous section. In the second regime, the current is non-uniformly distributed over the stages and each subsequent stage is operated at a lower current density (see Table 2).

Fig. 4a shows the current density (uniformly distributed) and the corresponding measured voltage over each stage for the multistage. Fig. 4b shows the corresponding concentrations of both the diluate and concentrate outlets per stage. Fig. 4c shows a non-uniformly distributed current density and the corresponding measured voltage for each stage in the multistage. Fig. 4d shows the corresponding concentrations of both the diluate and concentrate outlets per stage. For both regimes, the *average* current density applied to the stages was 75 A/m^2 and the feed flow velocity 10 mm/s.

Fig. 4a shows an increase in cell pair voltage per stage, while the applied current density is kept uniform over the stages. Fig. 4b shows a linear behavior over the different stages for both diluate and concentrate concentrations, which means that there is no significant water transport and a constant salt removal per stage. As the diluate concentration decreases steadily, the voltage increases with each stage due to the increased resistance associated with the lower salt concentration. Oppositely, Fig. 4c shows that when the applied current density is decreased in a subsequent stage also the corresponding cell pair voltages decrease. Fig. 4d shows that the outlet concentrations change accordingly to the applied current density per stage. Therefore, in the first stage more ions are transported from diluate to concentrate than in the latter stages. The electrical resistance of the diluate increases per stage, but since the current density at each stage is lowered even more, the voltage decreases with every stage. These measurements at non-uniform current density conditions show that it is possible to operate each stage at different current densities.

Fig. 5 shows the energy consumption for the multistage operation per stage at uniform current and non-uniform current distribution and the energy consumption for the single-stage. All configurations are operated at an *average* current density of 75 A/m^2 and a feed flow

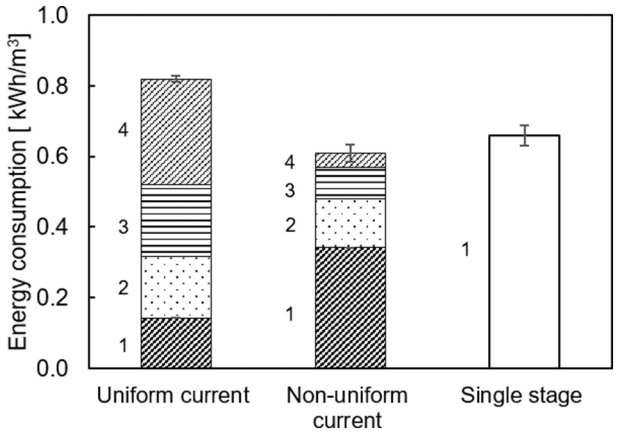

Fig. 5. Energy consumption plotted for the multistage configuration for uniform and non-uniform current distribution (patterned) and single-stage (empty). The numbers indicate the stage. All data obtained at an average current density of 75 A/m^2 and a feed flow velocity of 10 mm/s.

velocity of 10 mm/s.

Fig. 5 shows that the multistage configuration operating at uniform current density has an energy consumption that is 25% higher than that of the multistage configuration with non-uniform current distribution. The energy consumption for the multistage configuration with non-uniform current distribution is comparable to that of the single-stage configuration. In the multistage with uniform current distribution, the electrodes are all forced to transfer an equal current density. Because in the last stage, the concentration gradient is the highest, this results in a higher voltage and corresponding higher energy consumption, as can also be deducted from Fig. 4a. In contrast, multistage non-uniform current operation shows a higher energy consumption in the first stage, in analogy with Fig. 4c where both the current density and the voltage decrease with each stage. Interestingly, the multistage configuration with non-uniform current density distribution operates at a similar energy consumption as the single-stage configuration. When the energy consumption is comparable, the current distribution must be comparable between the single-stage and the non-uniform current distribution operated multistage configuration. This can be explained because migration of ions in ED follow the path of the least resistance, meaning that the highest (local) current density is found at the entrance of the single stage, accordingly to the high value for current density applied to the first stage in the multistage. As the energy consumption is very comparable between the single-stage and non-uniform distributed multistage for the desalination of 500 mM to 275 mM, in terms of energy consumption there is no benefit to use multistage.

4.3. Determination of limiting current density per stage and maximum desalination rate

In all cases discussed before, the diluate still contains ± 200 mM NaCl, while the WHO guideline for drinking water quality is < 8.5 mM [17]. The above-mentioned configurations are unable to reach such low values. Therefore, in this section we first determine the LCD value for each stage and subsequently adapt the operating current density for each stage to 95% of this LCD value to maximize the desalination degree in the multistage system.

The single stage configuration showed a LCD value at 10 mm/s of 130 A/m^2 or a current of 5.2 A. The desalination reached at these conditions at both outlets of the single stage were 857 mM and 123 mM. This confirms that full desalination in a single stage ED configuration is not possible.

Fig. 6 shows the LCD values per ED stage investigated for a multistage comprised of four stages and feed flow velocities ranging from 2.5 mm/s to 15 mm/s. Additionally, Fig. 6b shows the corresponding diluate and concentrate concentrations per ED stage for the multistage configuration with each stage operated at 95% LCD current density.

The LCD decreases with each stage in the multistage configuration (Fig. 6a), while the concentration in the diluate decreases and that in the concentrate increases (Fig. 6b). The reason is that due to the lower diluate concentration limiting current conditions are reached earlier. The decrease in LCD scales with the decrease in salt removal per stage. As a consequence, highest current densities and highest desalination degrees are observed in the first and the second stage (up to 600 A/m^2 in the first stage at a salt removal of 375 mM, and still 226 A/m^2 in the second stage at a salt removal of 163 mM), as at the initial stages the salt concentration is still relatively high. The third and fourth stages are only able to operate at very low LCD (< 1/10th of that of the first stage).

With increasing feed flow velocity, the LCD increases accordingly as well. The first two stages show that the LCD increases linearly with the feed flow velocity. However, in the third and fourth stage this is not applicable anymore due to the relatively low amount of salt.

In Fig. 6b the concentrate concentration increases mainly in the first stage, but the next stages do not show any further significant increase in salt concentration. At higher feed flow velocity, the concentration of the concentrate is higher as well. At lower feed flow velocities and therefore longer residence times and higher osmotic differences over the membrane, water transport from diluate to concentrate is higher, especially in the last two stages, resulting in a decrease in concentration for the lowest velocities. After four ED stages operating at 95% of the LCD value in each stage, the lowest diluate outlet concentration obtained is 11.4 mM, which comes close to the WHO target, i.e. 8.5 mM [17].

Fig. 7 shows the energy consumption and diluate concentration after four stages as function of the feed flow velocity ranging from 2.5 mm/s to 15 mm/s.

Fig. 7 shows an almost linear increase of the energy consumption with increasing feed flow velocity because energy dissipates at high salt removal rates at increased feed flow velocities. Simultaneously, however, Fig. 7 also shows that the diluate concentration after the fourth stage as function of feed flow velocity after the lowest flow velocity almost immediately reaches a constant value already at 5 mm/s. At the lowest feed flow velocity, the diluate concentration reached (38.2 mM) is still far off from the WHO target, due to the low flow velocity and consequently poor mixing in the diluate compartments at 2.5 mm/s. Increasing the feed flow velocity to 5 mm/s and higher results in reaching a constant diluate outlet concentration of about 11.5 mM, apparently reaching the limit in desalination degree of this specific multistage configuration.

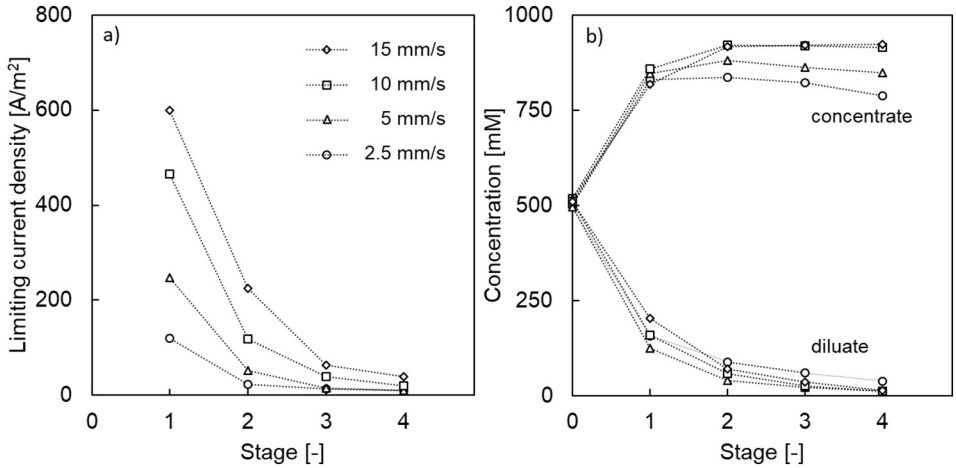

Fig. 6. Effect of feed flow velocity on: a) limiting current density found per ED stage, previous stages operated at 95% of their LCD; b) Outlet concentration per ED stage. The dashed lines are added to guide the eye.

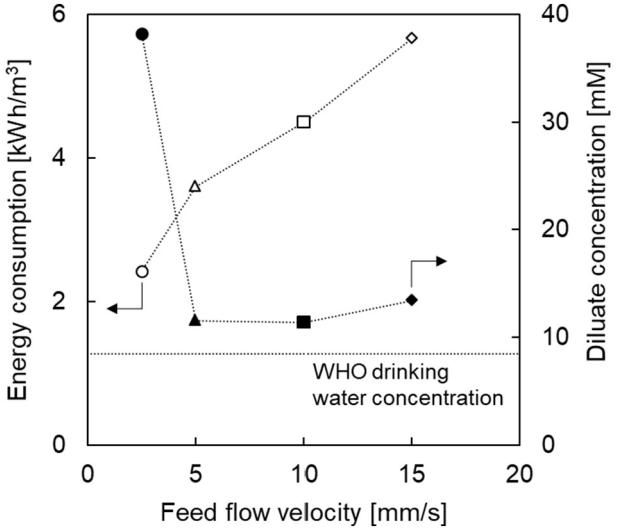

Fig. 7. Effect of feed flow velocity on energy consumption (open markers) and diluate concentration (solid markers) after four stages. The dashed line indicates the target concentration of 8.5 mM NaCl (target concentration for drinking water) [17]. The dashed lines are added to guide the eye.

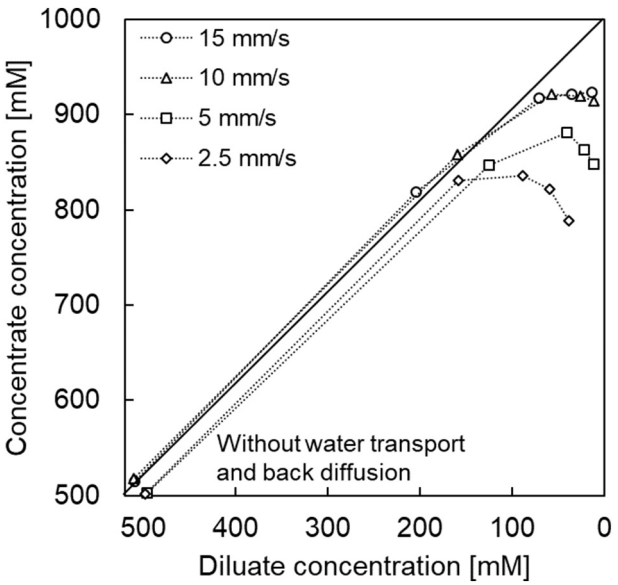

Fig. 8. Concentrate and diluate inlet concentration for stage 1 and outlet concentrate and diluate concentrations for each stage for a feed flow velocity ranging from 2.5 to 15 mm/s. The solid line describes ideal behaviour (i.e., without water transport and back diffusion), where the volume of the diluate and concentrate compartments do not change along the desalination degree. The dashed lines are added to guide the eye.

Fig. 8 shows the concentrate outlet concentration plotted against the diluate outlet concentration per stage of the multistage configuration for a feed flow velocity ranging between 2.5 mm/s and 15 mm/s.

In Fig. 8 the linear line describes membranes with ideal behaviour, meaning that there is no water transport associated to ion transfer. The points after the first stage are all close to ideal behaviour, indicating that in the first stage the effect of water transport and back diffusion is very small. At this first stage, the current density applied (Fig. 6a) and the concentration gradient between diluate and concentrate (Fig. 6b) is highest. Despite the high current density and large gradient over the membranes, the effect of water transport and back diffusion is small. In subsequent stages, where the current density is much lower compared to the first stage, the effect of electro-osmosis is negligible, however, as the gradient over the membranes between the diluate and concentrate increases up to 750–900 mM, water transport due to osmosis increases as well. This effect is clearly visible in Fig. 8 for at stage 2, 3 and 4, which show significant deviation from ideal behaviour. At higher feed flow velocities the effect of osmosis is less, as then the concentrate compartments do not decrease much in concentration.

This research shows that desalination of synthetic seawater close to drinking water is possible using multistage ED, but to reach this drinking water level at least 4 stages are needed. The energy consumption to desalinate close to drinking water levels is 3.6 kWh/m^3. A single stage ED with the same electrode area was not capable of this desalination degree. This means that the multistage ED requires not substantially higher capital expenditures, because the electrode area is the same. Only a few percent more membrane area is needed in the multistage to assure sealing. Staging will bring additional investment costs in piping, rectifiers and connections, but this is not significant. The energy consumption reached for a non-optimized multistage ED system is still double to state-of-the-art RO desalination technology. If the feed flow velocity in the multistage ED configuration is increased, similar diluate concentrations can be reached, but at a higher energy expenditure. To reach a product salinity that is lower than the WHO drinking water standard, the multistage configuration could be optimized for water transport and mixing in the diluate compartments. Once the water transport is lowered, the diluate yield a higher yield, and therefore a lower energy consumption is obtained. Once the mixing is increased, limiting current density values increases, and therefore higher desalination rates can be obtained. Such amendments to the multistage configuration will give no significant increase in energy consumption as the obtained diluate concentration is already close to the WHO drinking water standard.

5. Conclusions

The aim of this work is to compare single-stage ED to multistage ED and to desalinate synthetic seawater to drinking water concentrations at low energy consumptions. Salt and water transport are quantified for uniform current distribution in both configurations. The single-stage and the multistage show the same desalination performance for mild desalination i.e. salt removal of 300 mM. Non-uniform current distribution is investigated and shows the possibility of operating each stage at different current densities. Energy consumption for the non-uniform current distribution in the multistage shows a similar result to the single-stage configuration. For both single-stage and multistage configurations desalination to drinking water concentration is not possible in previous operations due to low applied current densities or due to LCD limitations. This shows that full desalination in a single-stage is not possible. Therefore, the maximum desalination degree per stage is assessed for the multistage by investigating the LCD per stage. Under all conditions, after the second stage, water transport becomes severe at low feed flow velocities. Despite this, with the multistage ED configuration operated at close to LCD conditions, synthetic seawater desalination from 500 mM to 11.4 mM, i.e. close to WHO drinking water standards at an energy consumption of 3.6 kWh/m^3 can be obtained. This is two times lower compared to previously reported energy consumptions for multistage ED [15] and comes closer to state-of-the-art RO desalination technology [2].

Acknowledgements

This work was performed in the cooperation framework of Wetsus, European Centre of excellence for sustainable water technology (www.wetsus.nl), within the REvivED project (Low energy solutions for drinking water production by a Revival of ElectroDialysis system), funded by the European Union's Horizon 2020 Research and Innovation program under Grant Agreement no. 685579 (www.revivedwater.eu). The authors would like to thank Hendrik Swart for performing the

multistage experiments for water and salt transport and Marrit van der Wal for carrying out the single-stage experiments and LCD multistage experiments.

References

[1] M. Shannon, P.W. Bohn, M. Elimelech, J.G. Georgiadis, B.J. Mariñas, A.M. Mayes, Science and technology for water purification in the coming decades, Nature 452 (2008) 301–310, https://doi.org/10.1038/nature06599.

[2] M. Elimelech, W.A. Phillip, The future of seawater desalination: energy, technology, and the environment, Science 333 (2011) 712–717, https://doi.org/10.1126/science.1200488.

[3] J.R. Werber, C.O. Osuji, M. Elimelech, Materials for next-generation desalination and water purification membranes, Nat. Rev. Mater. 1 (2016), https://doi.org/10.1038/natrevmats.2016.18.

[4] G. Amy, N. Ghaffour, Z. Li, L. Francis, R.V. Linares, T. Missimer, S. Lattemann, Membrane-based seawater desalination: present and future prospects, Desalination 401 (2017) 16–21, https://doi.org/10.1016/j.desal.2016.10.002.

[5] A.D. Khawaji, I.K. Kutubkhanah, J.M. Wie, Advances in seawater desalination technologies, Desalination 221 (2008) 47–69, https://doi.org/10.1016/j.desal.2007.01.067.

[6] T. Humplik, J. Lee, S.C. O'Hern, B.A. Fellman, M.A. Baig, S.F. Hassan, M.A. Atieh, F. Rahman, T. Laoui, R. Karnik, E.N. Wang, Nanostructured materials for water desalination, Nanotechnology 22 (2011), https://doi.org/10.1088/0957-4484/22/29/292001.

[7] S. Lin, M. Elimelech, Kinetics and energetics trade-off in reverse osmosis desalination with different configurations, Desalination 401 (2017) 42–52, https://doi.org/10.1016/j.desal.2016.09.008.

[8] C. Fritzmann, J. Löwenberg, T. Wintgens, T. Melin, State-of-the-art of reverse osmosis desalination, Desalination 216 (2007) 1–76, https://doi.org/10.1016/j.desal.2006.12.009.

[9] R.L. Stover, Seawater reverse osmosis with isobaric energy recovery devices, Desalination 203 (2007) 168–175, https://doi.org/10.1016/j.desal.2006.03.528.

[10] H. Strathmann, Electrodialysis, a mature technology with a multitude of new applications, Desalination 264 (2010) 268–288, https://doi.org/10.1016/j.desal.2010.04.069.

[11] A.M. Lopez, M. Williams, M. Paiva, D. Demydov, T. Duc, J.L. Fairey, Y.J. Lin, J.A. Hestekin, E.D. Edi, Potential of electrodialytic techniques in brackish desalination and recovery of industrial process water for reuse, Desalination 409 (2017) 108–114, https://doi.org/10.1016/j.desal.2017.01.010.

[12] R. Smith, Chemical Process Design and Integration, (2005), https://doi.org/10.1529/biophysj.107.124164.

[13] H. Strathmann, Ion-Exchange Membrane Separation Processes, (2004), https://doi.org/10.1007/s13398-014-0173-7.2.

[14] T. Seto, L. Ehara, R. Komori, A. Yamaguchi, T. Miwa, Seawater desalination by electrodialysis, Desalination. 25 (1978) 1–7, https://doi.org/10.1016/S0011-9164(00)82440-6.

[15] M. Turek, Cost effective electrodialytic seawater desalination, Desalination (2003), https://doi.org/10.1016/S0011-9164(02)01130-X.

[16] K.M. Chehayeb, K.G. Nayar, J.H. Lienhard, On the merits of using multi-stage and counterflow electrodialysis for reduced energy consumption, Desalination 439 (2018) 1–16, https://doi.org/10.1016/j.desal.2018.03.026.

[17] WHO, Guidelines for Drinking-water Quality, (n.d.).

[18] R.K. McGovern, A.M. Weiner, L. Sun, C.G. Chambers, S.M. Zubair, J.H. Lienhard V, On the cost of electrodialysis for the desalination of high salinity feeds, Appl. Energy 136 (2014) 649–661, https://doi.org/10.1016/j.apenergy.2014.09.050.

[19] Y. Tanaka, Ion-exchange membrane electrodialysis program and its application to multi-stage continuous saline water desalination, DES 301 (2012) 10–25, https://doi.org/10.1016/j.desal.2012.06.007.

[20] N. Lakshminarayanaiah, Transport Phenomena in Artificial Membranes, Chem. Rev. 65 (1965) 491–565, https://doi.org/10.1021/cr60237a001.

[21] G.W. Murphy, Osmionic demineralization, Ind. Eng. Chem. 50 (1958) 1181–1188, https://doi.org/10.1021/ie50584a042.

[22] A.A. Sonin, R.F. Probstein, A hydrodynamic theory of desalination by electrodialysis, Desalination 5 (1968) 293–329, https://doi.org/10.1016/S0011-9164(00)80105-8.

[23] V.V. Nikonenko, A.V. Kovalenko, M.K. Urtenov, N.D. Pismenskaya, J. Han, P. Sistat, G. Pourcelly, Desalination at overlimiting currents: state-of-the-art and perspectives, Desalination 342 (2014) 85–106, https://doi.org/10.1016/j.desal.2014.01.008.

[24] L. Han, S. Galier, H. Roux-de Balmann, Ion hydration number and electro-osmosis during electrodialysis of mixed salt solution, Desalination 373 (2015) 38–46, https://doi.org/10.1016/j.desal.2015.06.023.

[25] C. Jiang, Q. Wang, Y. Li, Y. Wang, T. Xu, Water electro-transport with hydrated cations in electrodialysis, Desalination 365 (2015) 204–212, https://doi.org/10.1016/j.desal.2015.03.007.

[26] M. Tedesco, H.V.M.V.M. Hamelers, P.M.M. Biesheuvel, Nernst-Planck transport theory for (reverse) electrodialysis: II. Effect of water transport through ion-exchange membranes, J. Memb. Sci. 531 (2017) 172–182, https://doi.org/10.1016/j.memsci.2017.02.031.

[27] M. La Cerva, L. Gurreri, M. Tedesco, A. Cipollina, M. Ciofalo, A. Tamburini, G. Micale, Determination of limiting current density and current efficiency in electrodialysis units, Desalination 445 (2018) 138–148, https://doi.org/10.1016/j.desal.2018.07.028.

[28] D.A. Cowan, J.H. Brown, Effect of turbulence on limiting current in electrodialysis cells, Ind. Eng. Chem. 51 (1959) 1445–1448, https://doi.org/10.1021/ie50600a026.

[29] A.H. Galama, M. Saakes, H. Bruning, H.H.M. Rijnaarts, J.W. Post, Seawater predesalination with electrodialysis, Desalination 342 (2014) 61–69, https://doi.org/10.1016/j.desal.2013.07.012.

[30] J. Veerman, J.W. Post, M. Saakes, S.J. Metz, G.J. Harmsen, Reducing power losses caused by ionic shortcut currents in reverse electrodialysis stacks by a validated model, J. Memb. Sci. 310 (2008) 418–430, https://doi.org/10.1016/j.memsci.2007.11.032.

[31] J.W. Post, H. Huiting, E.R. Cornelissen, H.V.M. Hamelers, Pre-desalination with electro-membranes for SWRO, Desalin. Water Treat. 31 (2011) 296–304, https://doi.org/10.5004/dwt.2011.2400.